LA-UR-14-24087
Approved for public release; distribution is unlimited.

Title:	Uranium and plutonium prompt-fission-neutron spectra (PFNS) from the analysis of NTS NUEX data and the corresponding uncertainty budget
Author(s):	Lestone, John P. Shores, Erik F.
Intended for:	To transmit prompt-fission neutron energy spectra uncertainty budget information to uncleared staff in T-division.
Issued:	2014-06-06

LA-UR-14-xxxxx

Uranium and plutonium prompt-fission-neutron spectra (PFNS) from the analysis of NTS NUEX data and the corresponding uncertainty budget

J. P. Lestone and E. F. Shores
XCP-3, Los Alamos National Laboratory
June 3rd, 2014

I. Introduction

For the past three decades, the theoretical standard that many experimentalists have compared their measured prompt-fission-neutron spectra (PFNS) to is the Los Alamos fission Model (LAM) of Madland and Nix [1]. The parameters in the LAM have been since updated by tuning to additional data that became available in the 1990s (most notably those of Staples *et al*. [2]). LAM calculations exist for ^{235}U(n,f), ^{238}U(n,f) and ^{239}Pu(n,f) reactions for incident-neutron energies from 0 to 20 MeV and for outgoing fission-neutron energies from 0 to 30 MeV. These calculations form the basis for the ENDF/B-VII [3] PFNS for the three main actinides.

Traditional methods for measuring PFNS use pulsed neutron beams from accelerator facilities. PFNS are generally inferred by measuring the time-of-flight of neutrons from tagged fission events in small mass targets, to neutron detectors typically ~1-2 meters away [2,4,5]. Assumed PFNS play a critical role in the simulation of the reactivity of critical systems. The yields of isotopes generated by high-energy threshold (n,xn) reactions are very sensitive to the details of the high energy tails of the PFNS. For these reasons, experiments that can test the LAM are of great interest to the nuclear data community. This is done in the present paper by inferring PFNS from NUEX data obtained from several underground US nuclear explosions conducted at the Nevada Test Site (NTS).

This release is an update to previous releases [6,7] and contains additional information on the uncertainty budget. Error terms not included previously are added to the analysis. These additional error terms do not significantly change the uncertainty budget for all but a few points.

II. NTS neutron experiment (NUEX)

The neutron experiment (NUEX) was a common diagnostic on nuclear device tests conducted at the Nevada Test Site. In these experiments neutrons from a device pass up a collimated line of site, and in the case of a Faraday cup (FC) NUEX, the neutrons pass through a thin CH_2 foil. Some of these neutrons interact with the nuclei in the foil, generating light charged particles (predominately protons) which are collected in a Faraday cup. The time dependence of the Faraday cup current is a measure of the energy spectrum of the neutrons that leak from the device. With good device models and accurate neutron-transport codes, the leakage spectrum can be converted into a prompt fast-neutron-induced fission-neutron energy spectrum (PFNS) from ~1 to 12 MeV. This has been done for two events containing a plutonium primary, where the NUEX data

were of a particularly high quality, and one event containing a uranium primary. The fission-neutrons in the device were produced by fission events induced by neutrons over a broad range of energies. We have listed the inferred 1.5-MeV n + ^{239}Pu fission-neutron spectrum in Table 1 for outgoing neutron energies from 1.5 to 11.5 MeV, in 1-MeV steps. The uranium device contained a larger high explosive charge. This limited the extraction of the uranium PFNS to neutron energies < 10 MeV. The listed values represent the fission-neutron emission probability at the quoted outgoing neutron energies and are not the integrals over 1-MeV wide bins. The quoted relative emission probabilities are all relative to the probability of emitting 1.5-MeV neutrons. The presence of the high explosive charge surrounding the fissile material made estimates of the lower energy PFNS (below 1 MeV) problematic. To obtain estimates of the absolute emission probabilities, the low-energy portion of the PFNS was assumed to be as calculated by the Los Alamos (fission) model [1]. The two NUEX inferred PFNS are labeled Pu-NUEX; and U-NUEX. Pu-NUEX was obtained by a combination of Pu-NUEX-1and Pu-NUEX-2 [6,7]. Pu-NUEX-1 was from an event near the end of US nuclear testing and its data quality was higher than the data associated with the earlier events used to obtain Pu-NUEX-2 and U-NUEX.

Table 1. Pu-NUEX : inferred PFNS for 1.5-MeV neutron induced fission of ^{239}Pu; and the ratio of the NUEX inferred spectrum to the Los Alamos model (LAM).

Neutron energy (MeV)	Relative emission Probability	Probability (1/MeV)	LAM (1/MeV)	Probability ÷ LAM
1.5	1.000±0.025	0.2905±0.0073	0.2907	0.999±0.025
2.5	0.670±0.017	0.1945±0.0049	0.1913	1.017±0.025
3.5	0.382±0.010	0.1110±0.0028	0.1099	1.011±0.025
4.5	0.209±0.005	0.0607±0.0015	0.0603	1.005±0.025
5.5	0.110±0.003	0.0318±0.0010	0.0323	0.985±0.030
6.5	0.0573±0.0020	0.0166±0.0006	0.0169	0.986±0.035
7.5	0.0294±0.0014	0.00853±0.00039	0.00862	0.990±0.046
8.5	0.0145±0.0012	0.00421±0.00035	0.00434	0.970±0.080
9.5	0.0077±0.0009	0.00224±0.00026	0.00217	1.03±0.12
10.5	0.0047±0.0009	0.00135±0.00027	0.00108	1.25±0.25
11.5	0.0010±0.0011	0.00029±0.00032	0.00053	0.55±0.61

Table 2. U-NUEX : inferred PFNS for 1.5-MeV neutron induced fission of ^{235}U; and the ratio of the NUEX inferred spectrum to the Los Alamos model (LAM).

Neutron energy (MeV)	Relative emission Probability	Probability (1/MeV)	LAM (1/MeV)	Probability ÷ LAM
1.5	1.000±0.025	0.2947±0.0074	0.2921	1.009±0.025
2.5	0.639±0.016	0.1884±0.0047	0.1903	0.990±0.025
3.5	0.361±0.009	0.1063±0.0028	0.1050	1.013±0.026
4.5	0.190±0.005	0.0559±0.0015	0.0554	1.009±0.027
5.5	0.0940±0.0037	0.0277±0.0011	0.0286	0.969±0.038
6.5	0.0487±0.0023	0.0144±0.0007	0.0144	0.997±0.047
7.5	0.0216±0.0024	0.00638±0.00071	0.00706	0.90±0.10
8.5	0.00989±0.0021	0.00292±0.00061	0.00340	0.86±0.18
9.5	0.00309±0.0021	0.00091±0.00061	0.00163	0.56±0.37

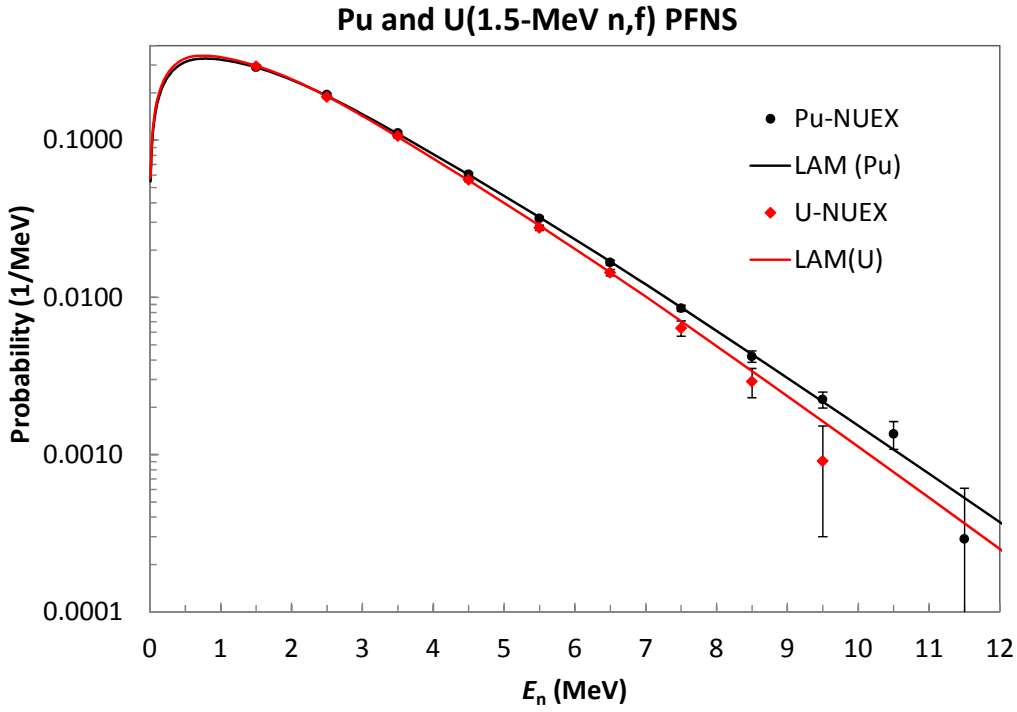

Fig. 1. The emission probabilities listed in Tables 1 and 2, and the corresponding 1.5-MeV n + ^{239}Pu and ^{235}U Los Alamos fission model PFNS [1] (curves).

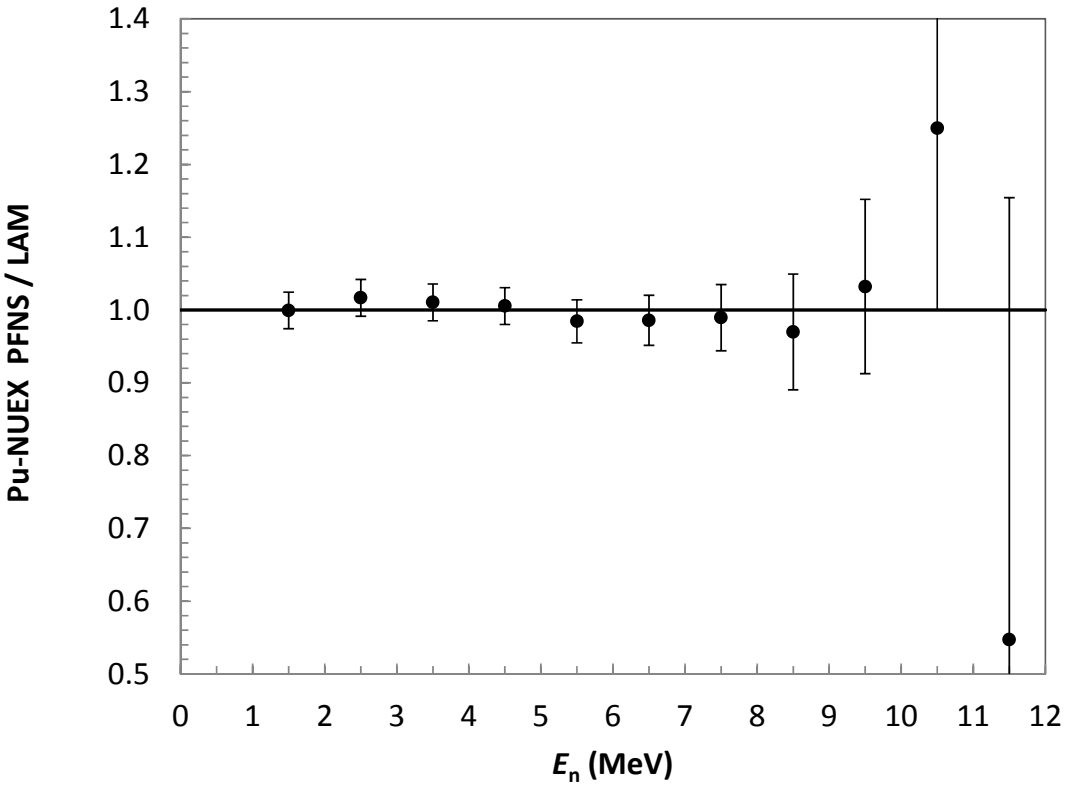

Fig. 2. Ratio of the Pu-NUEX inferred ^{239}Pu(1.5-MeV n,f) PFNS to the Los Alamos fission model (see Table 1).

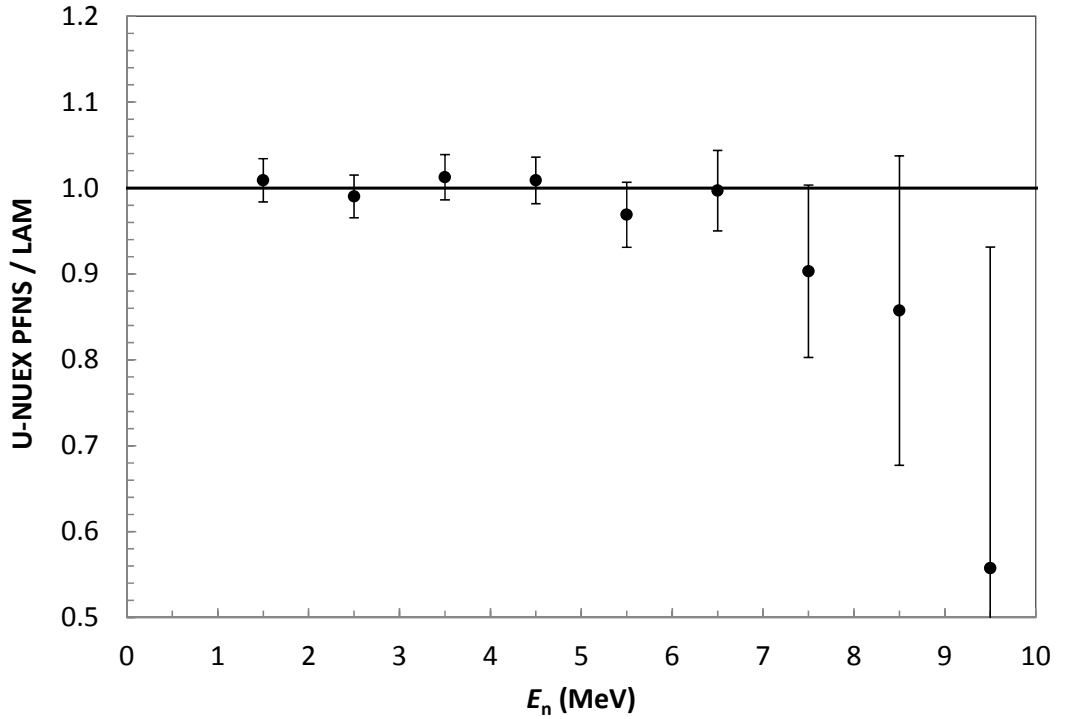

Fig. 3. Ratio of the U-NUEX inferred ^{235}U(1.5-MeV n,f) PFNS to the Los Alamos fission model (see Table 2).

There are common systematic uncertainties associated with both the Pu-NUEX and U-NUEX which cancel if the ratios of these two results are taken. These ratios are thus a good test of the Los Alamos fission model. Fig. 4 compares the ratio of Pu-NUEX to U-NUEX results to the corresponding ratios from the Los Alamos fission model.

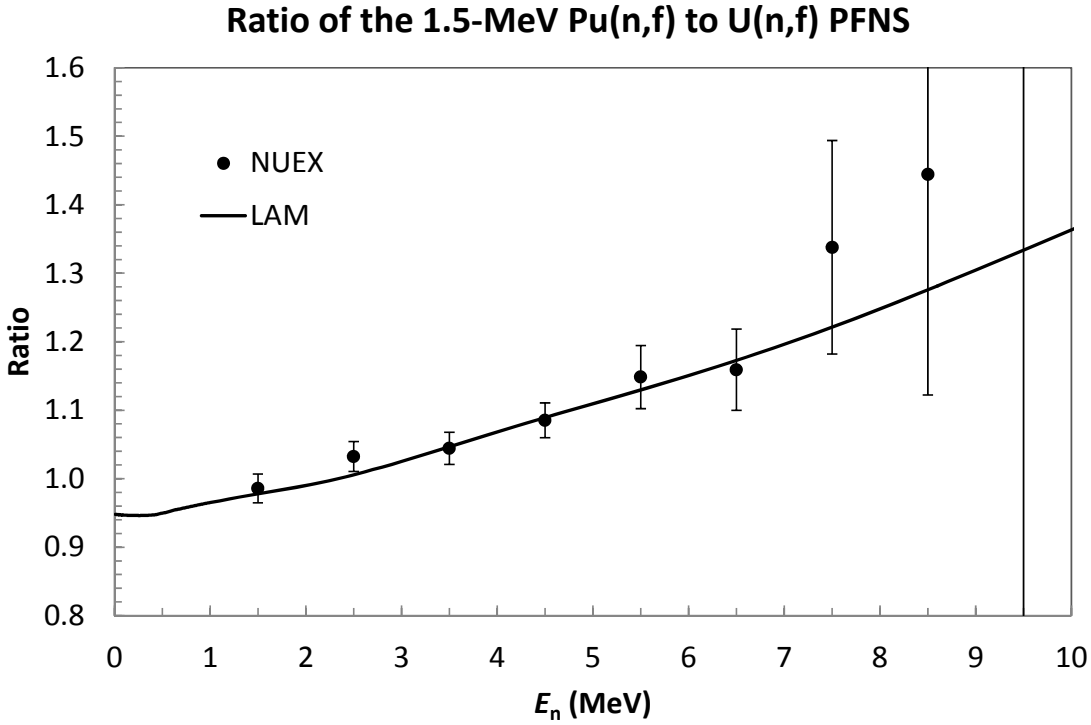

Fig. 4. A comparison of the ratio of Pu-NUEX to U-NUEX PFNS results to the corresponding ratios from the Los Alamos fission model (LAM).

III. Uncertainty budget

To understand the uncertainty budget in detail one needs to take into account some of the properties of boosted primaries, the complexities of how NUEX detectors convert neutron fluxes to current, and how these complexities are simulated in our codes. Figure 5 shows a schematic drawing of a NUEX setup. A NUEX is essentially a time-of-flight experiment. The 14-MeV fusion neutrons arrive first, generating the NUEX fusion peak, followed by the slower fission neutrons. Fission neutrons below 7 MeV are abundant and sufficiently after the fusion peak that the uncertainty analysis is relatively straightforward. However, for high-energy fission neutrons, the analysis is made complex by the presence of the fusion peak (see figure 6). The uncertainties in the inferred strengths of fission neutrons increase rapidly as the fission-neutron energy increases above ~8 MeV because this inference requires an accurate modeling of the shape of the fusion peak. This, in turn, requires an accurate knowledge of the location in time, size, and shape of the NUEX fusion peak, which requires a good model of, and other experimental constraints on, the time dependence of the fusion burn, the scattering of fusion neutrons to lower energies, and the production of charged particles exiting the NUEX CH_2 foil via the (n,p), (n,α), (n,3α), (n,^{12}C), and (n,^{12}C*) reactions. The scattering

of protons by the (n,p) reaction is very well understood and is the dominant source of charged particles incident on the Faraday cup (see figure 5). However, high-energy fusion neutrons interact with the carbon in the NUEX conversion foils generating small numbers of alpha-particles and ^{12}C ions. These alpha-particles and ^{12}C ions have velocities that are slower than the recoiling protons and arrive at the Faraday cup later, generating a significant current in the region between the fusion and fission peaks.

Eight sources of uncertainty have been identified and estimated for the inferred NUEX PFNS listed in Tables 1 and 2. These sources of uncertainty are listed and described below, tabulated in Tables 3 and 4, and displayed in figures 7 and 8.

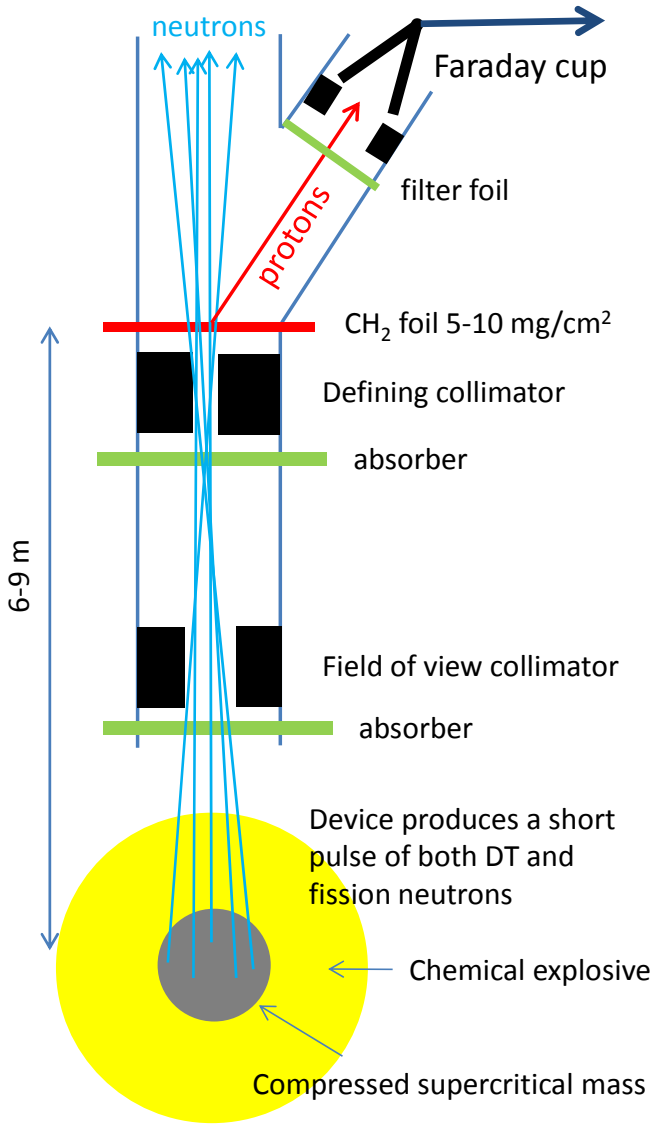

Fig. 5. Schematic representation of a NUEX setup.

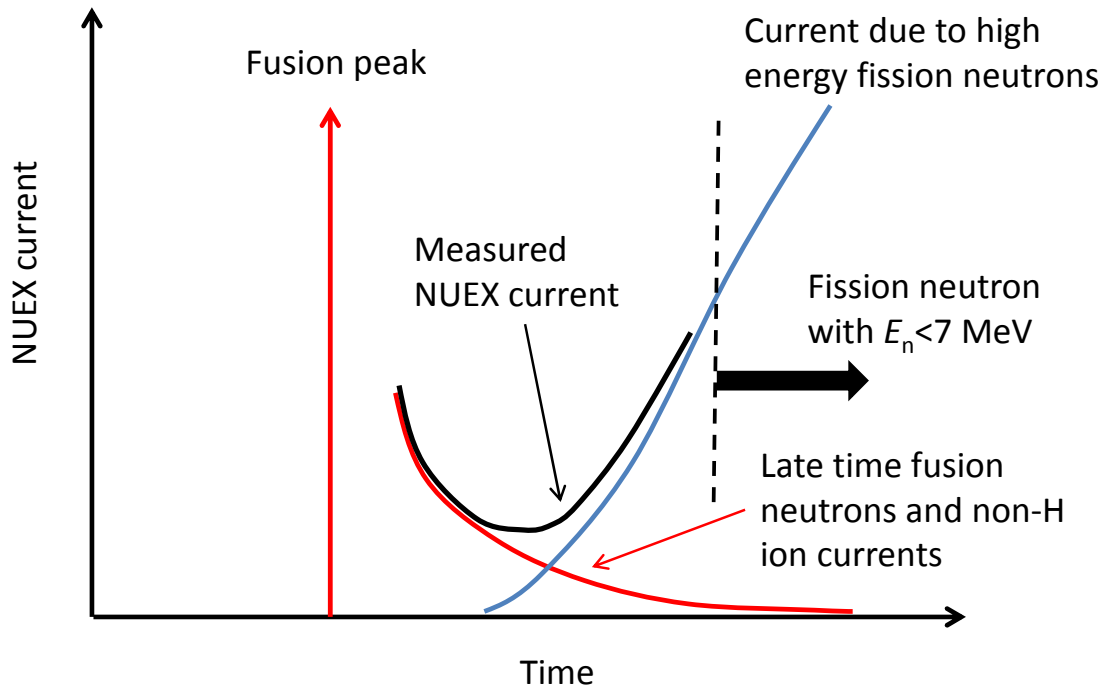

Fig. 6. Schematic representation of the NUEX current in the valley region between the fusion and fission peaks.

(1) The first and simplest uncertainty is due the uncertainties in the measured NUEX currents. This uncertainty is random between PFNS points.

(2) Cross sections and device geometry at nuclear time. This is the most difficult uncertainty term to quantify and justify in an unclassified setting. By comparing NUEX inferred results to other types of underground test (UGT) data and by assuming the cross-section and device-geometry corrections do not increase with increasing neutron energy, this uncertainty was determined to be ~2%. This is consistent with the scattering of the NUEX inferred PFNS about the LAM for neutron energies below ~5 MeV. This uncertainty is likely to contain only very weak correlations between neighboring PFNS points.

(3) Non-H ions from (n,α), (n,3α), and (n,^{12}C) reactions. The simulation of the generation of non-H ions, their transport through and out of the CH_2 foils, and their transport into the Faraday cup is more complex than the corresponding simulation of the proton collection. The relevant cross sections and angular distributions are not as well-known as for (n,p) scattering. There are additional complexities associated with calculations of the charge-state distribution of the ^{12}C ions that exit the CH_2 foil. Errors associated with the current generated by non-H ions are likely to be correlated across PFNS energy bins. However, it is possible that this error changes sign more than once across the energy region from 8 to 12 MeV. Fortunately for the Pu-NUEX, both thick- and thin-foil data exist. The lower energy, higher charge and mass of the alpha-particles and C ions, translate into short stopping lengths in the CH_2 foils. The alpha-particle and C-ion

currents are thus only generated by interactions between the neutron flux and the side of CH_2 foils facing the Faraday cup. The non-H ion currents are thus very similar for both thick (~10 mg/cm^2) and thin (~5 mg/cm^2) CH_2 foils while the proton currents due to high-energy fission neutrons scattering in thick foils are double that of the corresponding currents from thin foils. Any bias associated with errors in the simulated currents due to non-H ions can thus be removed by subtracting the thin-foil inferred PFNS from twice the thick-foil result. However, this subtracting procedure can greatly increase uncertainties and is only performed when inferring the Pu-NUEX PFNS at fission-neutron energies above 8 MeV where the thin-foil inferred PFNS is biased ~10% high relative to the corresponding thick-foil result. For fission-neutron energies below 8-MeV there is no evidence of a bias between the thick- and thin-foil results and the final results are obtained by a simple averaging.

(4) There are uncertainties associated with our simulation of the late-time dependence of the fusion peak due to uncertainties in the late-time dependence of the fusion burn and the down scattering of fusion neutrons to lower energies. The late-time dependence of the fusion burn can be constrained by an analysis of thresholded NUEX data which is a measure of the time dependence of the fusion burn. This is the dominant uncertainty associated with the late-time dependence of the fusion peak for the Pu-NUEX PFNS. The U PFNS was extracted from an earlier UGT with a thicker explosive charge. In this case, the dominant uncertainty is due to down-scattered fusion neutrons that arrive later than the main fusion peak. These uncertainties have correlations across neighboring PFNS points. It is possible that the sign of this error will change once across the relevant energy range.

(5) An uncertainty in the absolute magnitude of the fusion peaks of ~1% leads to significant uncertainties in the inferred PFNS at fission neutron energies above ~8 MeV, especially for the Pu-NUEX PFNS where the subtraction method is used to remove bias associated with the non-H ion currents (see uncertainty #3). This error is highly correlated across the inferred PFNS points.

(6) An uncertainty in the absolute timing of the fusion peaks of ~0.5 ns leads to significant uncertainties in the inferred PFNS at fission neutron energies above ~8 MeV, especially for the Pu-NUEX PFNS where the subtraction method is used to remove bias associated with the non-H ion currents (see uncertainty #3). This error is highly correlated across the inferred PFNS points.

(7) Monte Carlo errors in the simulated time dependence of the fusion peak leads to significant uncertainties in the inferred PFNS at fission-neutron energies above ~8 MeV, especially for the Pu-NUEX PFNS where the subtraction method is used to remove bias associated with the non-H ion currents (see uncertainty #3). This error is not correlated across the inferred PFNS points.

(8) The raw PFNS inferred from boosted primaries contains predominately fission-neutrons generated by events induced by fission neutrons, with a much smaller component due to fissions induced by higher-energy fusion neutrons. The fission-neutrons generated by events induced by fusion neutrons leads to a slight hardening of the observed leakage neutron spectrum measured by the NUEX detectors, relative to what would be observed if no fusion neutrons were present. To obtain an inferred PFNS due to only fission events induced by fission neutron the influence of the harder U and Pu (14-MeV n, *f*) is removed. This is done by assuming our best estimates of (14-MeV n, *f*) PFNS are as calculated with the LAM with the inclusion of a generous uncertainty. The mix of fusion and fission neutrons in a device is highly constrained by both radiochemical detectors and device models. Uncertainties associated with the removal of the contributions due to fission events induced by high-energy fusion neutrons are strongly correlated across PFNS points. Although unlikely, we cannot rule out that the sign of this error may change across the relevant energy range.

Table 3. Pu-NUEX uncertainty budget.

	Uncertainty number (%)								
E_n (MeV)	1	2	3	4	5	6	7	8	total
1.5	0.6	2.0						1.2	2.5
2.5	0.6	2.0						1.2	2.5
3.5	0.6	2.0			0.1	0.2	0.1	1.3	2.5
4.5	0.6	2.0			0.1	0.4	0.1	1.4	2.5
5.5	0.6	2.0	0.1	0.1	0.1	0.8	0.1	1.9	3.0
6.5	0.6	2.0	0.3	0.1	0.2	1.2	0.2	2.5	3.5
7.5	0.8	2.0	0.9	0.2	0.4	1.6	0.5	3.6	4.6
8.5	2.7	2.0		1.1	1.1	5.1	1.3	5.1	8.2
9.5	4.0	2.0		3.2	2.2	6.9	2.6	6.8	11.6
10.5	7.4	2.0		11.2	5.6	8.5	5.1	8.6	20
11.5	33	2.0		98	30	10.5	26	10.7	110

Table 4. U-NUEX uncertainty budget.

	Uncertainty number (%)								
E_n (MeV)	1	2	3	4	5	6	7	8	total
1.5	0.8	2.0						1.3	2.5
2.5	0.8	2.0						1.2	2.5
3.5	0.8	2.0			0.1	0.1	0.1	1.4	2.6
4.5	0.8	2.0		0.8	0.1	0.4	0.1	1.3	2.7
5.5	0.8	2.0	0.1	2.9	0.1	0.8	0.1	1.1	3.9
6.5	0.8	2.0	0.4	3.6	0.2	1.2	0.2	1.6	4.7
7.5	1.0	2.0	1.2	10.3	0.5	1.6	0.6	2.6	11.1
8.5	1.2	2.0	3.0	20	0.5	2.2	1.1	4.1	21
9.5	1.8	2.0	7.0	66	1.0	2.7	2.3	5.8	67

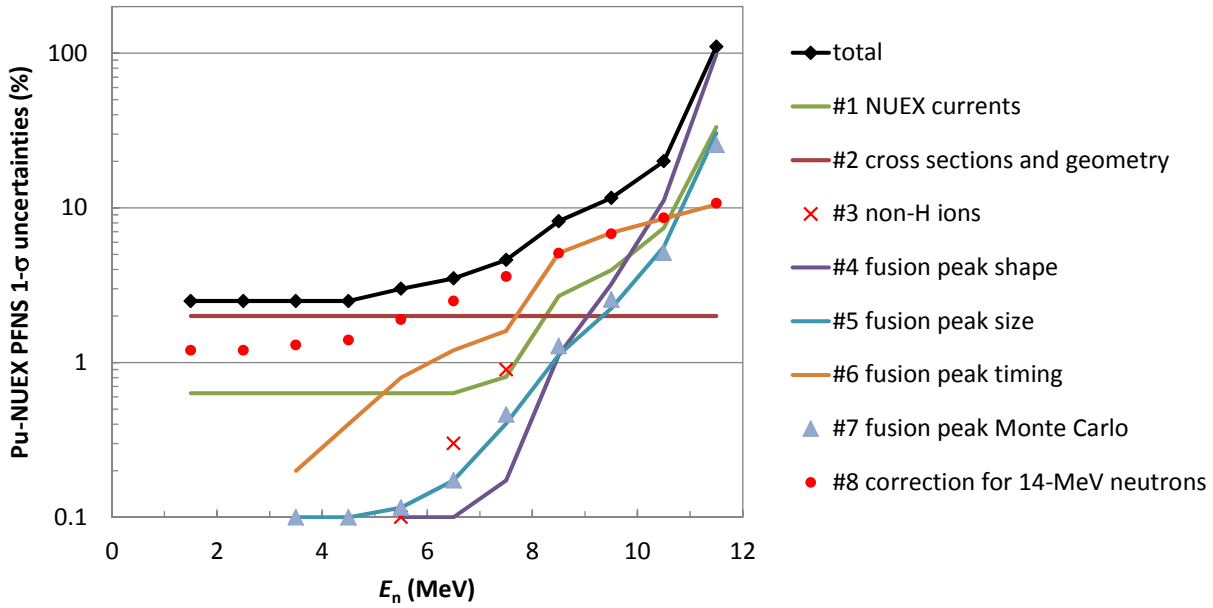

Fig. 7. Pu-NUEX uncertainty budget.

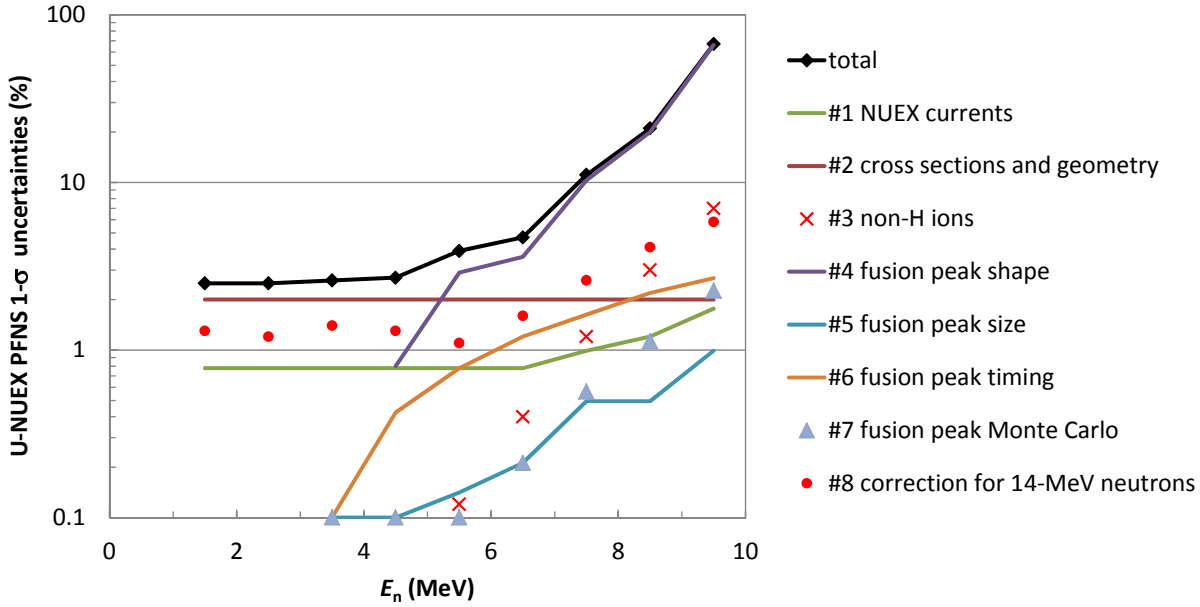

Fig. 8. U-NUEX uncertainty budget.

IV. Summary and Conclusions

Prompt-fission-neutron-spectra have been inferred from Nevada-Test-Site nuclear tests from two plutonium devices, and one uranium device. The 1.5-MeV ^{239}Pu(n,f) PFNS is inferred from ~1 to 12 MeV. The 1-σ error bars are less than 3% up to fission-neutron energies of 6 MeV, less than 5% up to fission-neutron energies of 8 MeV, and less than 20% up to fission-neutron energies of 11 MeV. The 1.5-MeV ^{235}U(n,f) PFNS is inferred from ~1 to 10 MeV. The 1-σ error bars are less than 3% up to fission-neutron energies of 5 MeV, less than 5% up to fission-neutron energies of 7 MeV, and are less than ~20% up to fission-neutron energies of ~9 MeV. The ^{239}Pu-NUEX and ^{235}U-NUEX inferred PFNS, and their ratio, are in agreement with the LAM.

[1] D. G. Madland and J. R. Nix, Nucl. Sci. and Eng. **81**, 213 (1982), and http://t2.lanl.gov/data/fspect.
[2] P. Staples *et al*. Nucl. Phys. A **591**, 41 (1995).
[3] M. B. Chadwick *et al*. Nucl. Data Sheets, **112**, 2887 (2011).
[4] S. Noda *et al*. Phys. Rev. C **83**, 034604 (2011).
[5] P. I. Johansson and B. Holmquist, Nucl. Sci. Eng., **62**, 695 (1977).
[6] J. P. Lestone and E. F. Shores, Los Alamos National Laboratory Report, LA-UR-13-21239 (2013).
[7] J. P. Lestone and E. F. Shores, Nucl. Data Sheets, **119**, 213 (2014).